Z. Phys. Chem. **226** (2012) 889–899 / **DOI** 10.1524/zpch.2012.0278

$La_{0.6}Sr_{0.4}CoO_{3-\delta}$ (LSC) Thin Film Electrodes with Very Fast Oxygen Reduction Kinetics Prepared by a Sol-Gel Route

By Judith Januschewsky[1], Michael Stöger-Pollach[2], Frank Kubel[1], Gernot Friedbacher[1], and Jürgen Fleig[1,*]

[1] Institute of Chemical Technologies and Analytics, Vienna University of Technology, Getreidemarkt 9-164/EC, 1060 Vienna, Austria
[2] University Service Centre for Transmission Electron Microscopy, Vienna University of Technology, Wiedner Hauptstraße 8–10, 1040 Vienna, Austria

In memory of Professor Dieter Kolb

(Received May 25, 2012; accepted August 4, 2012)
(Published online September 10, 2012)

Solid State Electrochemistry / Oxygen Reduction / Lanthanum Cobaltite / Impedance / Microelectrode

$La_{0.6}Sr_{0.4}CoO_{3-\delta}$ (LSC) thin film electrodes of about 80 nm thickness were prepared via a sol-gel route on yttria-stabilized zirconia (YSZ) and gadolinium doped ceria (GDC) solid electrolytes. Impedance measurements on microelectrodes fabricated from these films revealed very low polarization resistances for electrochemical oxygen exchange at intermediate temperatures (500–600 °C). Prerequisite for the very fast oxygen reduction kinetics was a limitation of the preparation (annealing) temperature to 600 °C. Already after *ca.* 15 minutes annealing of the sol-gel prepared layer at this temperature, electrodes were electrochemically highly active despite low crystallinity (almost XRD amorphous). LSC electrodes on GDC showed much higher polarization resistances. However, this originated from an additional interfacial resistance rather than from kinetically slow LSC surfaces.

1. Introduction

For highly efficient and clean electricity production, solid oxide fuel cells (SOFCs) are a very attractive alternative to conventional combustion engines. One problem still limiting the efficiency of SOFCs is the electrochemical performance of the cathode, particularly when operating at lower temperatures. Promising candidates as cathode materials for 500–700 °C are mixed ionic and electronic conducting perovskite-type oxides such as lanthanum strontium cobaltite (LSC), lanthanum strontium ferrite (LSF)

* Corresponding author. E-mail: j.fleig@tuwien.ac.at

and cathodes including both Fe and Co (LSCF). However, the oxygen reduction kinetics taking place on those cathodes is quite complex and still not fully understood [1,2]. For detailed mechanistic studies on the electrode kinetics, simplification of the electrode/electrolyte system is highly recommended. One possibility to simplify the electrochemical systems is the restriction to thin film model electrodes. Those electrodes can be prepared by pulsed laser deposition (PLD) and radio frequency sputtering (see *e. g.* Refs. [3–16]), or by different wet chemistry routes such as sol-gel techniques [17–26].

Recent work on LSC and LSCF thin film electrodes revealed much information on the location of rate-limiting steps (surface or interface) [15,27,28]. It could also be shown [16] that the polarization resistance of $La_{0.6}Sr_{0.4}CoO_{3-\delta}$ thin film model electrodes deposited by PLD between 350 and 500 °C is two to three orders of magnitude smaller than for films deposited and annealed at much higher temperatures [15]. Resistance values as low as 0.1 Ω cm^2 at 600 °C could be achieved. Owing to the low deposition temperature, these thin film electrodes were more or less XRD-amorphous. A correlation between crystallinity and resistance and also between crystallization and degradation behavior was observed [16]. This raises the question, whether such low polarization resistance values can also be achieved by simpler and cheaper preparation methods such as a sol-gel route. In Refs. [25,26] excellent performance of nanoporous and nanocrystalline LSC thin films deposited via sol-gel methods were reported: When being measured by means of a porous LSCF current collector, very small resistances (partly much below 0.1 Ω cm^2) were found at 600 °C.

In this work, we prepared LSC thin film electrodes via a simple sol-gel route with the aim to achieve a similarly high performance for thin films without any extended porous current collectors and to determine how far substrate and annealing conditions affect the properties of such sol-gel prepared films. Spin coating was used to deposit the sol on different yttria stabilized zirconia (YSZ) and gadolinia doped ceria (GDC) substrates. The films were only partially crystallized during annealing at temperatures up to 700 °C for some minutes. Electrodes were characterized by impedance spectroscopy (IS), X-ray diffraction (XRD), scanning electron microscopy (SEM), transmission electron microscopy (TEM) and atomic force microscopy (AFM).

2. Experimental

2.1 Preparation of the thin films

$La_{0.6}Sr_{0.4}CoO_{3-\delta}$ (LSC) thin films were prepared from the metal-organic precursor materials lanthanum acetate [$La(CH_3COO)_3 \cdot 1.5H_2O$] (Alfa Aesar), strontium acetate [$Sr(CH_3COO)_2 \cdot 0.5H_2O$] (Alfa Aesar) and cobalt acetate [$Co(CH_3COO)_2 \cdot 4H_2O$] (Alfa Aesar). 0.27 g Co-acetate, 0.21 g La-acetate and 0.08 g Sr-acetate were dissolved in 3.5 ml glacial acetic acid which results in a Co-concentration of 0.29 mol/l. An amount of 0.038 g polyvinylalcohol was added in order to stabilize nanostructures. Addition of 100 pl formamid reduced the reactivity of the metal components and the whole mixture was kept for 2 hours at 80 °C in an ultrasonic bath. Then further 100 pl formamid were added. Thin films were prepared from this sol by spin coating on single-crystalline (1 0 0) oriented YSZ substrates (9.5 mol% Y_2O_3, CrysTec GmbH, Germany), on

pressed, sintered and polished YSZ polycrystals (8 mol% Y_2O_3, Tosoh, Japan), and on GDC (10 mol% Gd_2O_3, Treibacher, Austria) polycrystalline substrates. An amount of 0.1 ml of the sol was deposited on the substrates at 6000 rpm for 33 seconds spinning time. The resulting films were dried at 180 °C for 3 minutes, pre-annealed at 360 °C for 3 minutes and annealed at 500, 600 or 700 °C for another 3 minutes. For all thin films the procedure of spin coating and heat treatment was repeated once in order to get thicker films. The second layer has to be deposited after the entire heat treatment to avoid removal of parts of the first layer during preparation. This is in accordance with reports on lanthanum manganite thin films [29].

2.2 Characterization of the thin films

The structure of the sol-gel prepared thin films was determined on an X'Pert PRO diffractometer PW 3050/60 (Philips) in Bragg–Brentano geometry by Cu-Kα radiation. For scanning electron microscopy (SEM) measurements (FEI Quanta 200 FEGSEM), the thin films were coated by 510 nm gold to avoid local charging. Atomic force microscopy (AFM) was performed on a NanoScope 111 multimode SPM from Digital Instruments (Veeco Metrology Inc.). Information on the film microstructure was gained in tapping mode under ambient air using single-crystalline silicon cantilevers. Transmission electron microscopy (TEM) images were obtained on a FEI TECNAI F20 and G20.

For impedance measurements, the thin films were micro-structured into circular microelectrodes of 60 μm diameter by photolithography and argon ion beam etching [16]. The samples were placed on a heating stage, heated to 500 °C or 600 °C and contacted by gold-coated steel needles. Impedance spectra were measured in ambient air by an Alpha-A high performance frequency response analyzer (Novocontrol) in the frequency range from 10^6 to 10^{-1} Hz with an amplitude of 20 mV. The first impedance measurements were made immediately after heating to 500 °C, *i. e.* the only heat treatment was film annealing for 3 minutes at 500–700 °C (see Sect. 2.1). (The bottom layer of the two-layered films was six minutes at the corresponding annealing temperature.) Then the temperature was kept for 15 minutes at 600 °C and impedance spectra were continuously measured. Finally the temperature was reduced to 500 °C and impedance spectra were continuously recorded for 3 days.

3. Results and discussion

3.1 Structural and morphological characterization

After annealing at 600 °C or 700 °C for 3 minutes and also after additional 15 minutes at 600 °C the films did not show any signal of LSC in the diffraction pattern. After 3 days at 600 °C, however, diffraction peaks of rhombohedral (pdf #87-1081, R-3c) LSC can be observed (Fig. 1). The diagram in Fig. 1 was obtained by calibration and subtraction of two measurements, one after 3 minutes at 600 °C and one after 3 days at this temperature. The regions from 30 to 32° and 34 to 41° were excluded and linearized as they correspond to the single-crystalline YSZ substrate. The LSC thin film shows a preferential orientation along (1 0 0) and (1 1 0) in a hexagonal setting. Hence, we conclude that

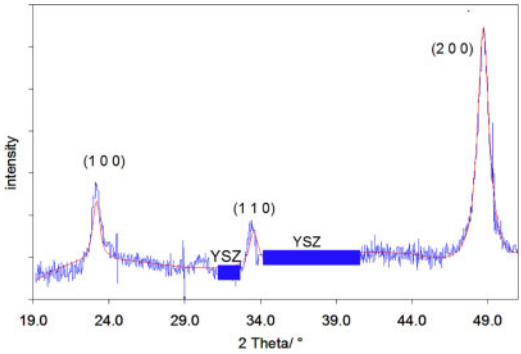

Fig. 1. Difference of two diffraction patterns of a LSC electrode (two sol-gel deposited layers) annealed at 600 °C for 3 minutes and then kept at 600 °C for another three days; the linearized regions correspond to the single-crystalline YSZ substrate.

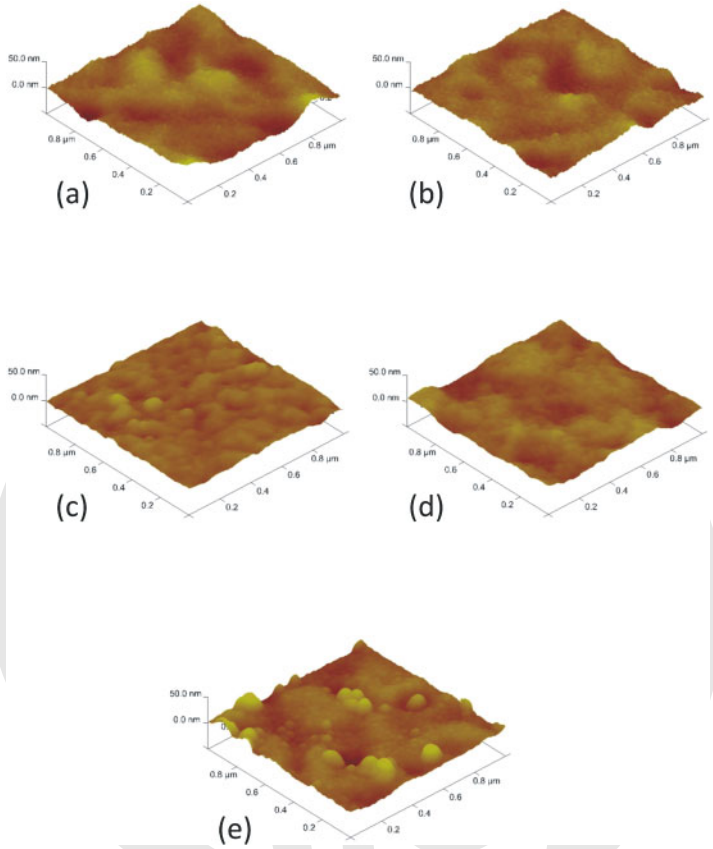

Fig. 2. AFM images of two-layered LSC electrodes annealed for 3 minutes at 500 °C **(a)** and 700 °C **(b)**, and of one **(c)** and two **(d)** sol-gel prepared layers annealed for 3 minutes at 600 °C. **(e)** AFM image of a LSC electrode consisting of two sol-gel prepared layers annealed at 500 °C for 3 minutes after 3 days at 500 °C.

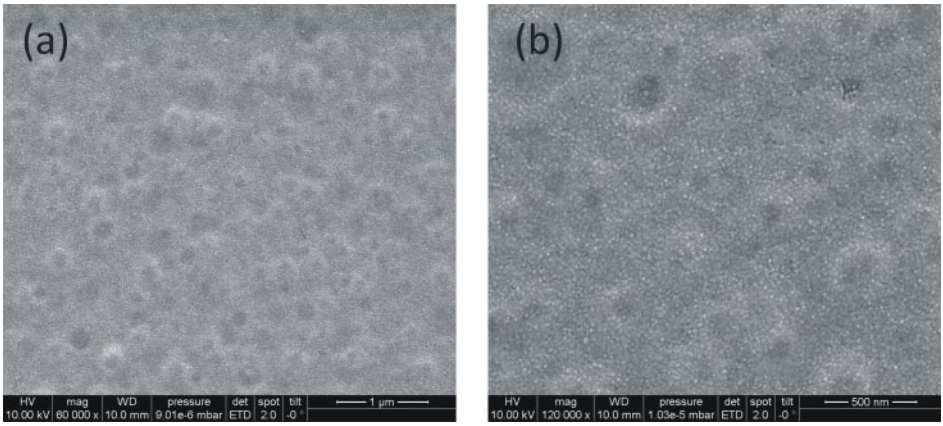

Fig. 3. SEM images of LSC electrodes consisting of one **(a)** and two **(b)** sol-gel prepared layers, each annealed at 600 °C for 3 minutes.

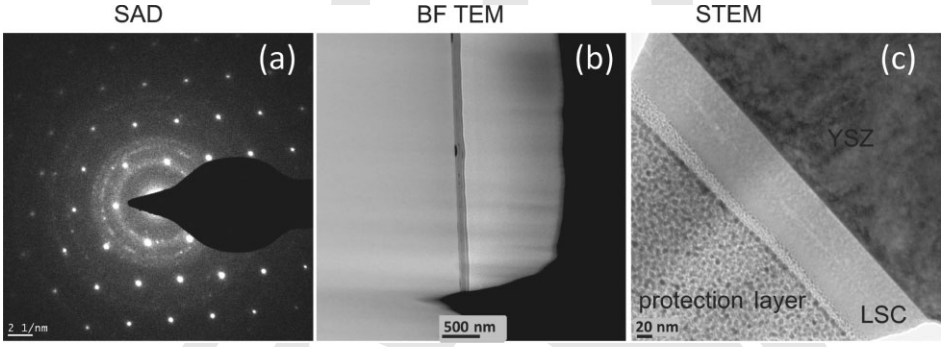

Fig. 4. (a) SAD pattern of a (two-layered) LSC electrode annealed for 3 minutes at 600 °C; **(b)** bright field image and **(c)** STEM image of the same sample.

the thin films are XRD amorphous after short annealing but crystallize during the heat treatment at 600 °C.

AFM images of two-layered thin films annealed for 3 minutes at 500 °C (Fig. 2a), 700 °C (Fig. 2b) and 600 °C (Fig. 2d) are shown, respectively. The rms roughnesses of all two-layered films are between 3.5 and 6 nm and do not differ significantly for different annealing temperatures. After sol-gel processing of only one layer, the annealed film had a slightly lower roughness value of 3 nm (Fig. 2c). Some differences between one- and two-layered thin films are also visible in SEM images (Fig. 3) with the two-layered thin film (Fig. 3b) being rougher. Long-term annealing (3 days) at 500 °C lead to the growth of cyrstals on the surface (Fig. 2e).

In the selected area diffraction (SAD) pattern (Fig. 4a) the sharp spots correspond to the single-crystalline YSZ substrate. The rings indicate amorphous and nanocyrstalline LSC. Bright field (BF) TEM images (Fig. 4b) and STEM images (Fig. 4c) reveal a con-

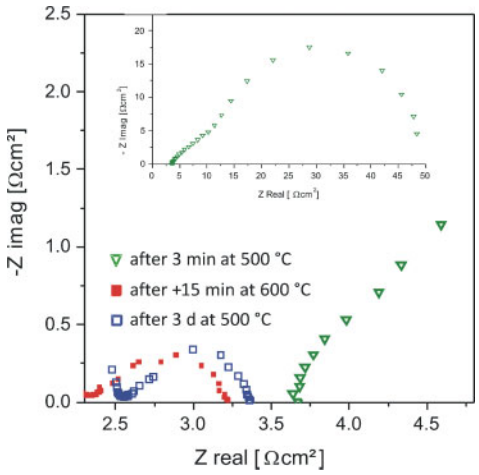

Fig. 5. Impedance spectra of LSC thin film microelectrodes on single-crystalline YSZ, annealed for 3 minutes at 500 °C and measured at 500 °C (the bottom layer of the two-layers film was 6 minutes at 600 °C, see Experimental): as prepared (green triangles, also shown in the inset), after additional 15 minutes at 600 °C (red filled squares), after additional 3 days at 500 °C (blue open squares). Resistances are normalized to the electrode area. The apparent difference of the electrolyte bulk resistance is most probably caused by an additional sheet resistance for lateral electron transport in thin film electrodes with very short annealing time.

stant thickness of the thin films over the entire width of the image. The interface between the two layers is still clearly visible with closed pores between the substrate and the first layer as well as between the first and second sol-gel prepared layer. Indication of open porosity was not found in TEM but existence of nano-pores can also not be excluded. The total film thickness is about 80 nm with one sol-gel layer exhibiting a thickness of 40 nm.

3.2 Electrochemical measurements

3.2.1 Impedance spectra

Depending on preparation and pre-history, mostly either one arc or two strongly overlapping arcs are visible on the complex impedance plane (Fig. 5). A reasonable separation into two resistances as in Ref. [15] (surface and interface) was not always possible and only the total electrode polarization resistance R_e will be considered in the following (exception: measurements on GDC substrates, see Sect. 3.2.4). Depending on the spectra, one or two R-CPE-elements (resistance R in parallel to a CPE = constant phase element) in series to an electrolyte bulk related resistance were used to parameterize the data. The total electrode resistance was either the fitted R-value (for one R-CPE-element) or the sum of the two resistive contributions to the total electrode resistance. Owing to this pragmatic approach also unambiguous interpretation of R_e in terms of its origin (surface, interface) is not possible. However, the capacitance deduced from the constant phase element (of the larger or the only electrode arc) with impedance

Table 1. Overview of the total electrode resistance R_e values of different samples measured at 500 °C and 600 °C.

Annealing temperature	Sample	Electrode resistance R_e in Ω cm² measured at 500 °C	600 °C	500 °C after 15 min at 600 °C	500 °C after 3 days at 600 °C
500 °C	LSC layer on single-crystalline YSZ	46.6	0.10*	0.81	1.12
600 °C	LSC layer on single-crystalline YSZ	54.6	0.15*	1.00	1.32
700 °C	LSC layer on single-crystalline YSZ	3.5	0.50	2.86	4.0
600 °C	LSC layer on polycrystalline YSZ	53.9	0.14*	1.60	1.59
600 °C	LSC layer on polycrystalline CGO	37.2	2.00*	8.8	11.6

* after 15 min

$Z_Q = Q^{-1}(i\omega)^{-n}$ (ω: angular frequency) using equation [30] $C = (R_e^{1-n} Q)^{1/n}$ had values in the mF/cm² range. It thus most probably reflects the chemical capacitance of the LSC film [15] and this strongly suggests that, in accordance with Refs. [15,27,28,31,32] the electrode resistance is mainly caused by the oxygen reduction process on the surface of LSC (exception for GDC, see Sect. 3.2.4). When measuring microelectrodes vs. an extended counter electrode, only the microelectrode contributes significantly to the electrode resistance [33]. Hence, the electrode resistance can directly be scaled to the surface area of the microelectrode.

3.2.2 Polarization resistance of LSC on single-crystalline YSZ at 500 °C

The first impedance spectra were measured at 500 °C immediately after preparation *i. e.* after 3 minutes at 500-700 °C (bottom layer of the two-layered film: 6 minutes). Resulting polarization resistances are summarized in Table 1. Electrodes on single-crystalline YSZ have resistance values of about 50 Ω cm² if annealed at 500 °C or 600 °C for 3 minutes (*cf.* Fig. 5). The thin film annealed at 700 °C for 3 minutes has a much lower electrode resistance of 3.5 Ω cm². All these resistance values are already smaller than those of LSC thin film electrodes prepared (PLD) and annealed at much higher temperatures [2]. However, after 15 minutes at 600 °C and cooling back to 500 °C the resistance values become even much smaller than before (Fig. 5), except for the sample first annealed at 700 °C: Samples originally annealed at 500 and 600 °C reached about 1 Ω cm² at 500 °C, see Table 1 and Fig. 5. (The apparent difference of the electrolyte bulk resistance in Fig. 5 is most probably caused by an additional sheet resistance for lateral electron transport in thin film electrodes with very short annealing time; this sheet resistance contributes to the high frequency intercept [34]). This also shows that the lowest resistance could be achieved for LSC layers never exposed to high temperature (700 °C). A similar phenomenon was reported for PLD deposited films [16]: High temperature deposited and thus more crystalline LSC thin films on YSZ exhibit higher polarization resistances compared to thin films prepared at lower temperature with lower crystallinity. Thin film electrodes show only little degradation of these extremely low resistances after 3 days at 500 °C (Table 1 and Fig. 5). In AFM images,

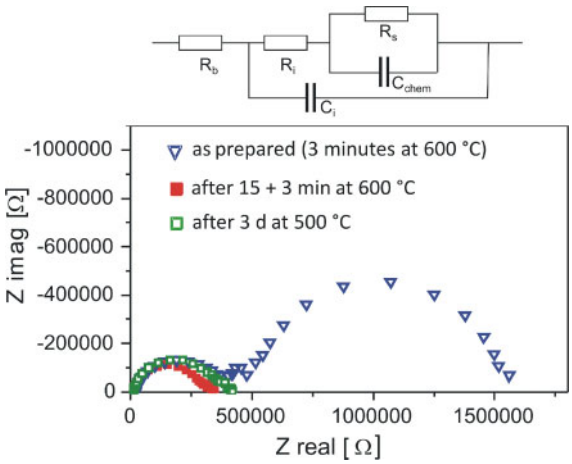

Fig. 6. Impedance spectra of LSC thin film microelectrodes on polycrystalline GDC measured at 500 °C. The film was annealed at 600 °C for 3 minutes (blue triangles, the bottom layer of the two-layers film was 6 minutes at 600 °C, see Experimental), annealed for additional 15 minutes at 600 °C (red filled squares), and kept 3 days at 500 °C (green open squares). Absolute resistance values are given for microelectrodes of 60 μm diameter.

a growth of crystals of about 200 nm in length is found after 3 days at 500 °C and it is unknown how far those are related to the minor degradation (Fig. 2e).

3.2.3 Polarization resistance of LSC on single-crystalline YSZ at 600 °C

During the first minutes at 600 °C the electrode resistance strongly decreases for the 500 °C and 600 °C prepared films. After some minutes at 600 °C all sol-gel thin films exhibit very low resistance values between 0.1 and 0.5 Ω cm^2 (see Table 1) with the thin film first annealed at 700 °C for 3 min having the highest resistance. This sequence is in accordance with the results at 500 °C. The electrode polarization resistances are again about two orders of magnitude lower than those reported for PLD films deposited and annealed above 700 °C [2] but comparable to those obtained for PLD films prepared at low deposition temperatures of 400–500 °C [16]. The results thus strongly suggest that the phenomenon of very low polarization resistances of LSC thin film electrodes is a matter of temperature prehistory rather than of the preparation method. Very low polarization resistances seem to be an "intrinsic" property of LSC thin film surfaces never being exposed to temperatures above approx. 600 °C. However, in a further study it could be shown that creation of very active surfaces by wet chemical etching, *i. e.* by uncovering a new "intrinsic" surface, is also possible, even for films prepared at higher temperatures [35]. This is probably related to removal of Sr-rich segregates formed during preparation, annealing or thermal degradation [35].

3.2.4 Polarization resistance of LSC on polycrystalline YSZ and GDC at 600 °C

After annealing at 600 °C for 3 + 15 minutes, thin films on polycrystalline YSZ have resistance values of 0.14 Ω cm^2 at 600 °C (Table 1). These and all values obtained at other

temperatures or annealing times show that there is no substantial difference in electrode polarization resistance between polycrystalline and single-crystalline YSZ. The LSC electrodes on polycrystalline GDC behave very differently. Minimum values of R_e achievable at 500 °C or 600 °C are about an order of magnitude higher than those on YSZ. This, however, does not necessarily mean that the corresponding LSC surface is electrochemically less active than on YSZ: For GDC, the spectrum shows two strongly separated arcs in the complex impedance plane when measured after preparation (3 minutes at 600 °C) (Fig. 6). The low frequency arc strongly shrinks during additional 15 minutes at 600 °C and ended as a hardly separable shoulder of the intermediate frequency arc which itself remains unchanged; the corresponding spectra measured at 500 °C are shown in Fig. 6. Further three days at 500 °C lead to little variation.

When fitting the very first spectrum by using the equivalent circuit shown in Fig. 6 and again calculating capacitances from the constant phase element (see above), we obtain a low frequency capacitance of 1–4 mF/cm^2. The data quality was not sufficient to still extract a low frequency capacitance from the slight shoulder of further annealed samples. According to literature the equivalent circuit in Fig. 6 is valid for an interplay of surface resistance R_s and interfacial resistance R_i with chemical capacitance C_{chem} and interfacial capacitance C_i; R_b denotes the serial electrolyte resistance. Several papers showed its applicability to mixed conducting thin film electrodes [15,27,32,36]. Since our result for the low frequency capacitance fits to values found for chemical capacitances, we suggest the intermediate frequency arc to be caused by an enhanced interfacial resistance (R_i). The hardly visible shoulder gives evidence that the resistance of oxygen reduction on the LSC surface R_s is again very small after 15 minutes at 600 °C and not fundamentally different from that on YSZ.

The large R_i value is quite surprising as usually YSZ rather than GDC is supposed to cause an interface resistance due to the formation of insulating zirconate between LSC and YSZ [37]. The very low interfacial capacitance suggests that a relatively thick layer at the GDC/LSC interface leads to the corresponding polarization resistance. Assuming a relative permittivity of 10–20 for this layer, it seems to be *ca.* 5–10 nm thick (calculated from C_i) and thus has a conductivity of about 10^{-7} $S\,cm^{-1}$. The origin of this resistive layer is not known yet, it might be a second phase but also LSC exhibiting different defect concentrations or different defect mobilities due to its growth on GDC; strain may play a role here. A similar phenomenon was also observed for LSC electrodes on GDC prepared by PLD [14].

4. Conclusions

lt was possible to prepare LSC sol-gel thin film electrodes on YSZ with very fast oxygen reduction kinetics. Resistance values as low as about 1 $\Omega\,cm^2$ at 500 °C and 0.1 $\Omega\,cm^2$ at 600 °C can be achieved. Prerequisite for such highly active layers is sufficiently low annealing temperature; 15 minutes at 600 °C was shown to be sufficient. A closely related effect was observed on PLD deposited films already before, suggesting that these properties are intrinsic features of LSC surfaces prepared at low temperatures. The electrolyte can strongly influence the polarization resistance of the LSC

thin film electrodes. On (single- as well as polycrystalline) YSZ, thin film electrodes have much smaller electrode resistances compared to thin films grown on polycrystalline GDC. This, however, is an effect of a yet to further identify resistive layer at the GDC/LSC interface.

References

1. S. B. Adler, Chem. Rev. **104** (2004) 4791.
2. F. S. Baumann, J. Fleig, G. Cristiani, B. Stuhlhofer, H. U. Habermeier, and J. Maier, J. Electrochem. Soc. **154** (2007) B931.
3. X. Chen, S. Wang, Y. L. Yang, L. Smith, N. J. Wu, B.-I. Kim, S. S. Perry, A. J. Jacobson, and A. Ignatiev, Solid State Ionics **146** (2002) 405.
4. D. Mori, H. Oka, Y. Suzuki, N. Sonoyama, A. Yamada, R. Kanno, Y. Sumiya, N. Imanishi, and Y. Takeda, Solid State Ionics **177** (2006) 535.
5. A. Bieberle-Huetter, M. Sogaard, and H. L. Tuller, Solid State Ionics **177** (2006) 1969.
6. D. Waller, L. G. Coccia, J. A. Kilner, and I. W. Boyd, Solid State Ionics **134** (2000) 119.
7. M. Mosleh, N. Pryds, and P. V. Hendriksen, Mater. Sci. Eng. B **144** (2007) 38.
8. M. Sase, J. Suzuki, K. Yashiro, T. Otake, A. Kaimai, T. Kawada, J. Mizusaki, and H. Yugami, Solid State Ionics **177** (2006) 1961.
9. S. Madhukar, S. Aggarwal, A. M. Dhote, R. Ramesh, A. Krishnan, D. Keeble, and E. Poindexter, J. Appl. Phys. **81** (1997) 3543.
10. D. Brodoceanu, A. Manousaki, I. Zergioti, A. Klini, M. Dinescu, and C. Fotakis, Appl. Phys. A: Mater. Sci. Proc. **79** (2004) 911.
11. H. D. Bhatt, R. Vedula, S. B. Desu, and G. C. Fralick, Thin Solid Films **350** (1999) 249.
12. M. Sase, F. Hermes, K. Yashiro, K. Sato, J. Mizusaki, T. Kawada, N. Sakai, and H. Yokokawa, J. Electrochem. Soc. **155** (2008) B793.
13. A. Endo, H. Fukunaga, C. Wen, and K. Yamada, Solid State Ionics **135** (2000) 353.
14. J. Januschewsky, M. Kubicek, M. Stöger-Pollach, J. Bernardi, and J. Fleig, ECS Transactions **25** (2009) 2397.
15. F. S. Baumann, J. Fleig, H.-U. Habermeier, and J. Maier, Solid State Ionics **177** (2006) 1071.
16. J. Januschewsky, M. Ahrens, A. Opitz, F. Kubel, and J. Fleig, Adv. Funct. Mater. **19** (2009) 3151.
17. V. V. Srdic, R. P. Omorjan, and J. Seydel, Mater. Sci. Eng. B **116** (2005) 119
18. J. Pagnaer, A. Hardy, D. Mondelaers, G. Vanhoyland, J. D'Haen, M. K. Van Bael, H. Van den Rul, J. Mullens, and L. C. Van Poucke, Mater. Sci. Eng. B **118** (2005) 79.
19. I. Zergioti, A. W. M. De Laat, U. Guntow, F. Hutter, and O. Maerten, Appl. Phys. A: Mater. Sci. Proc. **69** (1999) S433.
20. L. Dieterle, D. Bach, R. Schneider, H. Stoermer, D. Gerthsen, U. Guntow, E. Ivers-Tiffee, A. Weber, C. Peters, and H. Yokokawa, J. Mater. Sci. **43** (2008) 3135.
21. K.-S. Hwang, H.-M. Lee, S.-S. Min, and B.-A. Kang, J. Sol-Gel Sci. Techn. **18** (2000) 175.
22. B. J. Kim, J. Lee, and J. B. Yoo, Thin Solid Films **341** (1999) 13.
23. H. J. Hwang, A. Towata, M. Awano, and K. Maeda, Scripta Mater. **44** (2001) 2173.
24. G. Westin, M. Ottoson, and A. Pohl, Thin Solid Films **516** (2008) 4673.
25. J. Hayd, L. Dieterle, U. Guntow, D. Gerthsen, and E. Ivers-Tiffée, J. Power Sources **196** (2011) 7263.
26. C. Peters, A. Weber, and E. Ivers-Tiffee, J. Electrochem. Soc. **155** (2008) B730.
27. T. Kawada, J. Suzuki, M. Sase, A. Kaimai, K. Yashiro, Y. Nigara, J. Mizusaki, K. Kawamura, and H. Yugami, J. Electrochem. Soc. **149** (2002) E252.
28. Y. L. Yang, A. J. Jacobson, C. L. Chen, G. P. Luo, K. D. Ross, and C. W. Chu, Appl. Phys. Lett. **79** (2001) 776.
29. X. Zhu, S. Li, X. Yang, and J. Qiu, Appl. Surf. Sci. **254** (2007) 532.
30. J. Fleig, Solid State Ionics **150** (2002) 181.

31. N. Imanishi, Y. Sumiya, K. Yoshimura, T. Matsumura, A. Hirano, Y. Takeda, D. Mori, and R. Kanno, Solid State Ionics **177** (2006) 2165.
32. J. Jamnik and J. Maier, Phys. Chem. Chem. Phys. **3** (2001) 1668.
33. J. Fleig, H.-R. Kim, J. Jamnik, and J. Maier, Fuel Cells **8** (2008) 330.
34. V. Brichzin, J. Fleig, H.-U. Habermeier, G. Cristiani, and J. Maier, Solid State Ionics **152–153** (2002) 499.
35. M. Kubicek, A. Limbeck, T. Frömling, H. Hutter, and J. Fleig, J. Electrochem. Soc. **158** (2011) B727.
36. J. Fleig, F. S. Baumann, V. Brichzin, H.-R. Kim, J. Jamnik, G. Cristiani, H.-U. Habermeier, and J. Maier, Fuel Cells **6** (2006) 284
37. O. Yamamoto, Y. Takeda, R. Kanno, and M. Noda, Solid State Ionics **22** (1987) 241.